ELSEVIER

polymer

The influence of elastomer concentration on toughness in dispersions containing preformed acrylic elastomeric particles in an epoxy matrix

J. He[a], D. Raghavan[a,*], D. Hoffman[b], D. Hunston[c]

[a]*Polymer Science Division, Department of Chemistry, Howard University, Washington, DC 20059, USA*
[b]*The Dow Chemical Company, Midland, MI 48674, USA*
[c]*Polymer Division, National Institute of Standards and Technology, Gaithersburg, MD 20899, USA*

Abstract

The influence of toughener concentration on the fracture behavior of two-phase, rubber-toughened epoxy is studied. To vary the concentration without altering other morphological features, samples generated from dispersions of preformed rubber (acrylic) particles in liquid epoxy monomer are used. By diluting with different amounts of epoxy prior to cure, the toughener concentration can be varied over a wide range. Thermal and microscope studies support the assertion of a constant morphology. The fracture results show that the toughness increases to a maximum and then decreases as the concentration is increased. This suggests an optimum concentration of toughening. Micrographs of the initiation zone on the fracture surface at high concentrations of rubber show less deformation than the equivalent surfaces at lower concentrations. This is consistent with a toughening mechanism based on particles initiating yielding and plastic flow in the matrix. © 1999 Elsevier Science Ltd. All rights reserved.

Keywords: Acrylic; Dispersion; Epoxy; Fracture; Morphology; Preformed particles; Thermoset; Toughening

1. Introduction

Epoxy resins are widely employed as structural adhesives and as the matrix material for glass-, carbon- and polyamide-fiber reinforced composites because epoxies have excellent bulk properties such as modulus, tensile strength, glass transition temperature, creep resistance, etc. Like most thermosets, however, the highly amorphous and crosslinked nature of the cured epoxy produces an undesirable characteristic, i.e. epoxies are brittle and show poor resistance to crack growth. The technology to toughen a crosslinked epoxy resin without undue sacrifices in the desirable properties by the addition of elastomer particles is well known [1–7]. Over the past two decades, a wide variety of materials have been studied, but the most common system is the carboxyl terminated acrylonitrile butadiene (CTBN) elastomer–epoxy composite [1–7]. The addition of CTBN improves the toughness significantly. The concentration of additive in such systems is commonly given in phr, parts by mass of additive per 100 parts by mass of epoxy resin. Note that phr is simply 100 times the mass ratio (mr) of additive to epoxy. Increasing the concentration

of CTBN raises the fracture energy up to a maximum of 15–20 times that of the unmodified epoxy at about 23 phr (0.23 mr) CTBN [4,8]. Further additions of CTBN, however, result in significant reductions in fracture energy and other mechanical and thermal properties.

The CTBN–epoxy system is typical of many toughened thermosets in that the morphology is generated during cure. CTBN is low enough in molecular weight that it is compatible with the liquid epoxy monomer. When the system is cured, the epoxy polymerizes and the CTBN reacts with epoxy monomer to form a copolymer. As the molecular weights of the epoxy and the CTBN copolymer increase, their compatibility decreases until phase separation occurs. The reactions continue until a glassy material is obtained. The morphology depends on the cure reactions, cure cycle and concentration of CTBN [8,9]. For systems with improved toughness, the usual morphology is particles of CTBN–epoxy in the micrometer range dispersed in an epoxy matrix. Good phase separation is required to maintain bulk properties like the glass transition temperature of the matrix.

It is widely recognized that the toughness depends on the morphology (average particle size and size distribution), the volume fraction of the second phase, and the nature of

---

* Corresponding author.

the particles and matrix. Because these features are generated during cure, they are difficult to control and systematically vary. Consequently, structure–property studies have met with only limited success [8,10]. For example, in the CTBN–epoxy system cured with piperidine, toughness increases with added CTBN up to a concentration of 23 phr (0.23 mr). Unfortunately, both the volume fraction of the second phase and the average particle size increase over this range so it isn't possible to separate the roles of such features. As the CTBN concentration is increased above 23 phr, the toughness goes down. At about 23 phr, however, the morphology also changes. As the CTBN concentration increases, the particle–matrix structure disappears and is replaced by a phase separated mixture with no clear matrix or included phase. At higher concentrations a phase inversion is seen with epoxy particles in a CTBN–epoxy matrix. It has been speculated that the loss of morphology is responsible for the decrease in toughness at high concentrations, but this hypothesis has not been proven [8].

To address this problem, the approach taken here is to use a new material system that starts with preformed rubber particles [11–15]. The hope is that the particle size and size distribution will remain unchanged when the concentration is altered because the particles are already preformed. The use of preformed rubber particles to toughen a thermoset has been known for many years [11–19], but the potential of such systems for basic research studies has not been fully exploited. The advantage of the system used in this work is that the concentration of the second phase material can be varied over a wide range.

2. Background

The base material used here is a dispersion of acrylic particles dispersed in a liquid epoxy monomer [12–14]. A critical issue for such a dispersion is how to maintain stability until the system cures into a solid. In this case, grafted copolymer dispersant serves as a stabilizer. The grafted copolymer has two reactive segments, one which couples with the epoxy matrix and the other which couples with the acrylic rubber. The chemistry of coupling and the procedure for preparation of rubber particle dispersion in epoxy resin has been described previously [11–13,15] and is based on a two step procedure: (i) vinylization and (ii) vinyl polymerization. Fig. 1 illustrates the pathway for preparation of the rubber particles in epoxy resin by dispersion polymerization. The epoxy resin is reacted with functional vinyl monomer such as methacrylic acid to form a mono-vinyl ester. The mono-vinyl ester upon copolymerizing with other acrylic vinyl monomers, can produce a highly-grafted, polymeric structure. During the vinyl polymerization, the polymer develops a microstructure with the core containing no grafted epoxy while the exterior to the core contains the grafted epoxy. It has been found that by controlling the degree of grafting, the particle size of acrylic

elastomer in the epoxy dispersion can be controlled. Previous work has shown that for achieving good stability of acrylic rubber dispersions in epoxy, a large amount of grafting is necessary [11,12,15]. Furthermore, a large amount of grafting often results in the formation of small stable rubber particles in the epoxy matrix.

The investigation here uses a dispersion that has an average particle size of 0.5 μm in diameter. The stabilization is excellent so that even after a number of years storage, there is no visual evidence of non-uniformity in the dispersion. Nevertheless, the work here used a freshly prepared amount of the dispersion.

3. Experimental procedure[1]

3.1. Materials

The preformed rubber particle dispersion in liquid epoxy monomer was supplied by Dow Chemical. Designated XU-71790.04L, it is a commercial material made by a one-step process and consists of an epoxy monomer (mass fraction 59.55%) and preformed acrylic-rubber particles (mass fraction 40.45%). The acrylic rubber is a dispersion of poly(2-ethylhexyl acrylate-*co*-glycidyl methacrylate). Although, the acrylic-rubber particles have a dispersion of sizes, an average diameter of 0.5 μm has been reported in the literature [11–14]. The epoxy monomer was Tactix 123 LER, a diglycidyl ether of bisphenol A (DGEBA) type resin.

Tactix 123 LER was used to dilute the XU-71790.04L to achieve the desired acrylic rubber concentration in the epoxy. Unmodified epoxy (Tactix 123 LER) served as the control for the study. Piperdine was used as a curing agent for these systems.

### 3.2. Preparation of cured sample

To prepare the rubber modified epoxy samples, the acrylic rubber dispersion (XU-71790.04L) was hand mixed with the appropriate amount of epoxy (Tactix 123 LER) for 5–10 min. The mixture was degassed under vacuum in a Fisher Scientific Isotemp Vacuum Oven Model 281A at 50–60°C until frothing stopped (about 3 h). The mixture was allowed to attain room temperature and five parts by mass of the curative agent (piperdine) were added for each 100 parts by mass of the epoxy. The mixing of piperdine was done gently so as to minimize air entrapment. The mixture was immediately poured into the pre-heated mold and cured at 120°C for 16 h. The oven was then turned off and allowed to cool slowly to room temperature. This gave the samples a reproducible thermal history.

---

[1] Certain commercial materials and equipment are identified in this paper in order to specify adequately the experimental procedure. In no case does such identification imply recommendation or endorsement by the National Institute of Standards and Technology, nor does it imply necessarily that the items are the best available for the purpose.

Vinylization Reaction
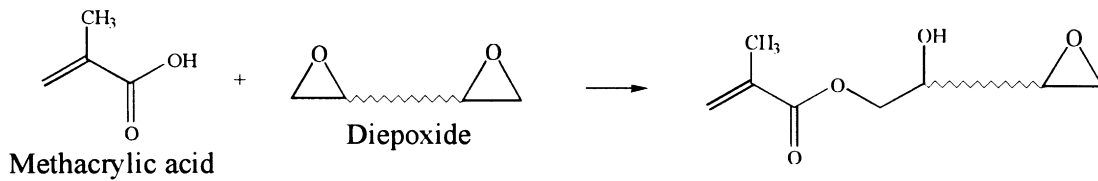
Vinyl Polymerization
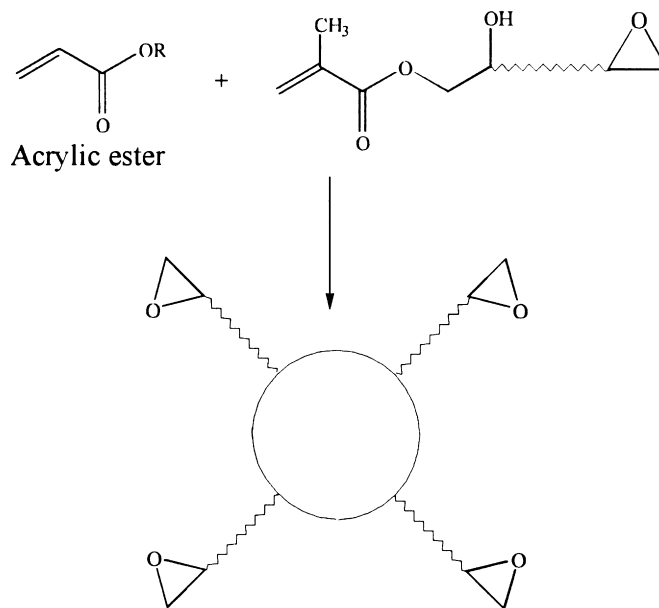
Stable Dispersion of Acrylic Elastomer in Epoxy Resin

Fig. 1. Reaction chemistry of rubber dispersed in epoxy resin.

The procedure used for the preparation of the unmodified epoxy specimens was similar to that of the modified epoxy except that only Tactix 123 and piperdine were used. The samples varied in color from brownish yellow to a creamy yellow depending on the rubber content in the cured specimen.

3.3. Preparation of compact tension and flexural bending specimens

The molding process produced plaques that are approximately 25 cm by 25 cm and 1.27 cm thick. The test specimens were cut from these plaques. The flexural moduli were determined in three-point bending (ASTM D-790) using rectangular bar specimens shown in Fig. 2a. The toughnesses were measured using a mode-I fracture test with compact tension specimens illustrated in Fig. 2b. The relative dimensions of the specimen were determined in general accordance with ASTM E-399. The specimen thickness was selected to assure that plane strain conditions would be present. A saw was used to create a notch through about 40% of the sample. A sharp precrack was then generated by placing a knife edge against the end of the notch and carefully tapping the back of the knife edge with a hammer until a sharp crack grew a short distance ahead. The knife edge was allowed to rest for 30 s before it was removed.

3.4. Flexural testing

The three-point bend experiments were conducted on an MTS 810 mechanical testing machine. At least three samples were tested at each concentration. Each bar was measured five times in one orientation and then rotated 90° about the length axis and tested five times in the second orientation. The sample was first loaded at a constant cross-head speed until the load was approximately equal to a predetermined value. The cross-head speed was selected to complete the loading in 10–20 s. The
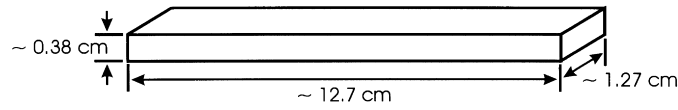
a: Bending Specimen
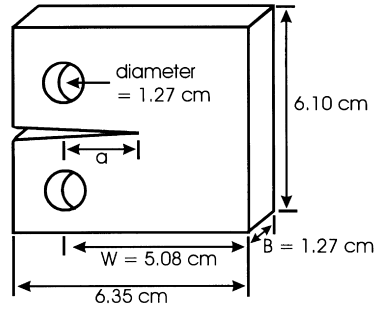
b: Compact Tension Specimen

Fig. 2. Test specimens.

deformation was then held constant for 290 s in a stress relaxation experiment. Finally, the sample was unloaded at the same cross-head speed used for loading. Through out the test, the load and cross-head position were monitored at 10 points per second and stored in a computer. Because the machine stiffness was very high, the data could be analyzed to determine the displacement of the sample at the central loading point, δ. This was combined with the load, P, to determine the bending modulus, $E(t)$, as a function of time in the range from the end of the loading step until just prior to the unloading step, $\sim$10–300 s.

$$E(t) = \frac{P(t)l^3}{4wh^3d} \tag{1}$$

$$d = \delta - \frac{3Pl}{8whG} \tag{2}$$

The span between the two outer supports (100 mm) is l, the specimen width and thickness are w and h, while G is the shear modulus. The second term on the right in Eq. (2) is a correction for the contribution of shear deformation [20]. Since G is unknown, E is first calculated with no correction. G is then estimated as $E/(2 + 2\nu)$, where ν is Poisson's ratio and is taken as 0.35 for epoxy. E is then computed using the estimated value of G. This procedure is repeated until the change in E per iteration is less than 0.01%. For all of the samples tested here, however, the shear correction produced only a minor change in E. The maximum tensile strain, ε_m,

in the sample occurs in the outer surface of the bar:

$$\varepsilon_m = \frac{6\delta h}{l^2} \tag{3}$$

To examine the linearity of the properties for these materials, one sample was tested six different times by loading to different initial load levels each time.

3.5. Fracture toughness studies

In order to determine the critical stress intensity factors, K_{IC}, and fracture energies, G_{IC}, the compact tension specimens were placed on a United Floor Model Electromechanical Testing Machine and loaded to failure at a constant cross-head displacement speed of 0.05 cm/min. The load, P, versus displacement, Δ, curves were recorded for 10 specimens at each rubber concentration. The experiments were conducted at room temperature (20–22°C) using a 5 kN load cell at scales between 10 and 50%. The values of the stress intensity factors, K_{IC} were calculated from

$$K_{IC} = \frac{P_f Q}{B\sqrt{W}} \tag{4}$$

where: P_f = critical load for crack growth, B = sample thickness, W = distance from center of loading holes to end of specimen (Fig. 2b), and Q = a geometry factor, given by

$$Q = \frac{\left[2 + \left(\frac{a}{W}\right)\right]\left[0.866 + 4.64\left(\frac{a}{W}\right) - 13.32\left(\frac{a}{W}\right)^2 + 14.72\left(\frac{a}{W}\right)^3 - 5.6\left(\frac{a}{W}\right)^4\right]}{\left[1 - \left(\frac{a}{W}\right)\right]^{\frac{3}{2}}} \tag{5}$$

where a = length of precrack measured from center of loading holes (Fig. 2). The equation is valid for ($0.2 < a/w < 1$), but values closer to 0.7 are preferred. For tests where the sample fails by rapid (unstable) crack growth, P_f is the load corresponding to the onset of this growth. When the sample fails by steady (stable) crack growth, P_f is the load necessary to maintain crack propagation.

The critical strain energy release rates, G_{IC} were calculated as follows:

$$G_{IC} = \frac{K_{IC}^2(1 - \nu^2)}{E} \qquad (6)$$

where ν is the Poisson's ratio (assumed to be 0.35) and E is the flexural modulus.

3.6. Differential scanning calorimetry

The Differential Scanning Calorimetric (DSC) experiments were conducted over a temperature range from −150 to 150°C. Typically, samples were cooled from room temperature to − 150°C at 10°C/min and heated from −150 to 150°C at a heating rate of 20°C/min. The first scan was ignored and the glass transition temperature of the epoxy was recorded from the second scan.

3.7. Microscopy studies

To examine failure mechanisms, the fracture surfaces were examined in the region of crack growth initiation. Sections of the fractured compact test specimens were mounted using Conductive Carbon Cement adhesive 30GM from Structural Probe Inc. Ultra Spec 90 MMLVC Sputter was used for depositing Au–Pd on the specimen. The fracture surfaces were then examined with a JEOL JSM-5300 Scanning Electron Microscope (SEM).

Microscopy is also a good tool for characterizing morphology. Pictures of the fracture surface are not ideal for this purpose, however, since the deformations that occur can obscure the microstructure. Consequently, for morphology studies, the samples were sectioned to thicknesses of approximately 100 nm in thickness at −100°C using a Leica AG Ultracut S Cryoultramicrotome. The thin-sections obtained were then exposed to RuO_4 vapors for 2 min, and examined in a Philips CM-12 TEM operating at 120 keV. Representative areas of selected samples were photographed at 15 000 × magnification. The resulting photographs clearly show the phase separated particles. Efforts were made to quantify the particle size and size distribution from the photographs, but unfortunately, the very high volume fraction of particles in many of the samples caused problems for the analysis method used in previous studies [11–15]. This challenge is the subject of future work, but qualitative interpretations of the pictures can be offered here.
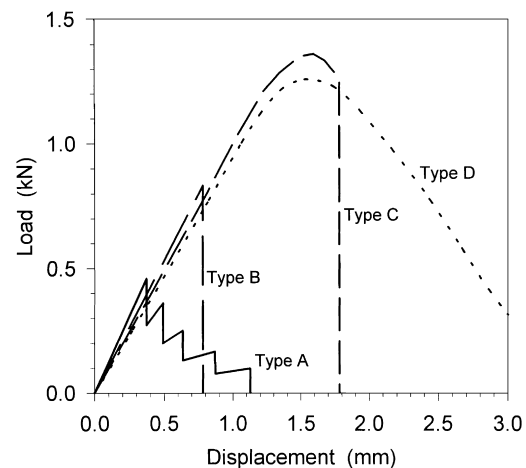

Fig. 3. Typical curves for fracture behavior of rubber-modified epoxies.

4. Results and discussion

4.1. Fracture studies of rubber-modified epoxy and unmodified epoxy

The crack growth behavior of the acrylic rubber-modified epoxies has been examined over a wide range of rubber concentrations. Over this range four basic types of load displacement behavior were noticed, and these were associated with different types of fracture behavior. Typical examples of the four load–deflection curves obtained are shown in Fig. 3. The Type A curve shown in Fig. 3 is the recorded load–displacement plot for a specimen that exhibits brittle unstable crack growth. The load increases linearly with displacement to a maximum value, at which point the crack propagates down the specimen in an unstable manner until the stored elastic energy is insufficient to produce further growth, and the crack arrests. The value of K_I or G_I at this point is sometimes called the arrest value. The process is repeated upon reloading of the specimen and ultimately the crack reaches the end of the specimen. This process is often characterized as slip/stick behavior. The length of the jumps in each crack propagation depends on a number of factors including the difference between the fracture energies for initiation and arrest. As that difference increases, the jumps get longer assuming that other factors don't change. The Type B curve shown in Fig. 3 is the recorded load–displacement plot for a specimen that exhibits unstable crack growth which leads to the complete failure of the specimen. Unlike Type A behavior, Type B curves do not show a slip/stick process. The load increases linearly with displacement to a maximum value, at which point the crack propagation results in catastrophic failure of the specimen. This generally means that the difference between the fracture energy for initiation of rapid crack growth is much larger than that associated with arrest, although other factors like machine stiffness may also be involved. The Type C curve shown in Fig. 3 is the recorded

Table 1
Fracture behavior of modified and unmodified epoxy system

| Acrylic rubber content		Representative type of fracture behavior	Percent of fracture surface with stress-whitening
(phr)	(mr)		
0	0	Type A	0
2.5	0.025	Type B	0.2–0.5
5	0.05	Type B	2–6
12.5	0.125	Type C	10–25
20	0.20	Type C	15–30
25	0.25	Type D	100
30	0.30	Type C/Type D	15–35/100
33	0.33	Type D	100
35	0.35	Type D	100
45	0.45	Type D	100
67	0.67	Type B	2–8

Fig. 4. Bending modulus as a function of deflection for a sample with 5 phr (0.05 mr) rubber. The dotted lines represent two standard uncertainties in the data.

load–displacement plot for a specimen that exhibits transition from stable crack growth to a unstable crack growth. The load increases linearly with deflection, but then becomes non-linear as the load approaches the maximum value. The crack growth is stable before and after the maximum load. Then there is a transition to a unstable crack growth. Much of the non-linearity in the load–displacement curve is associated with growth of the crack and not non-linearity in the mechanical properties of the material. For the toughest samples, however, significant deviations from linear elastic behavior are probably present. Since the fracture analysis assumes that the global behavior is linear elastic, this adds an additional uncertainty to the exact toughness values for those samples with the highest resistance to crack growth. The Type D curve shown in Fig. 3 is the recorded load–displacement plot for a specimen that exhibits stable crack growth. The crack growth is very stable producing a gradual failure. This behavior is often referred to as a driven crack since growth occurs only as long as the cross-head motion continues.

Table 1 summarizes the fracture behavior for various acrylic, rubber-toughened, epoxy systems. Generally, the samples with rubber content between 20 phr (0.2 mr) and 45 phr (0.45 mr) showed a more stable crack-growth behavior. Furthermore, it was noticed that the stress whitened region for these samples is much larger than that for epoxy samples containing 5 phr (0.05 mr) and 67 phr (0.67 mr) acrylic rubber. The fraction of the fracture surface that exhibited stress whitening is dependent upon the type of crack growth behavior. For Type A fracture, there was little or no stress whitening. With Type B fracture [observed for samples with 5 phr (0.05 mr) and 67 phr (0.67 mr) rubber], there was a distinct region of stress whitening (about 0.2–8% of the fracture surface) corresponding to the area just ahead of the crack tip at the onset of rapid crack growth. Beyond this region, the crack grew rapidly, and the fracture surface showed no stress whitening. Type D fracture behavior, on the other hand, produced stress whitening over the entire fracture surface [observed for samples with
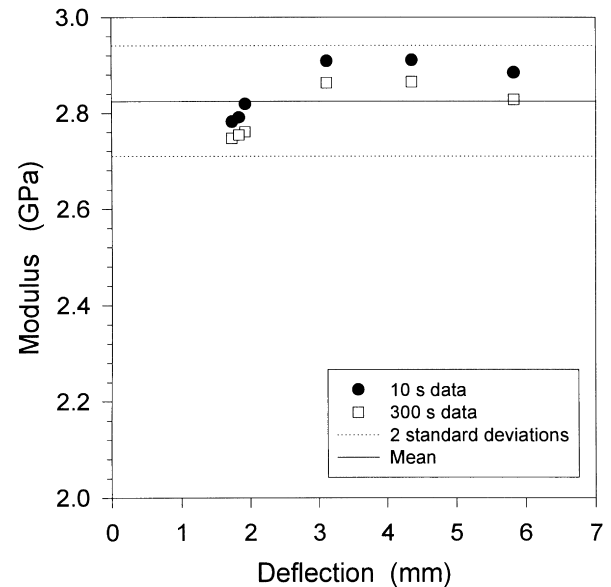
25 phr (0.25 mr), 30 phr (0.3 mr), 33 phr (0.33 mr), 35 phr (0.35 mr), and 45 phr (0.45 mr)]. As might be expected, Type C fracture behavior [observed for samples with 12.5 phr (0.125 mr) and 20 phr(0.2 mr)] had the characteristics of both Type B and D. The initial area of stable crack growth produced a continuous stress whitened surface like Type D fracture. When growth became unstable, the region just ahead of the crack tip was whitened, but beyond this, the rapid growth produced no whitening. The fraction of the fracture surface that was whitened varied from 10 to 35% depending on how long the crack growth remained stable. As the concentration of acrylic rubber was increased, there was a clear transition in fracture and stress whitening behavior from brittle unstable to stable and back to unstable.

4.2. Modulus data

It is well known that epoxies are viscoelastic so it is important that the appropriate modulus be used in calculating the fracture energies. One approach is to select the time-dependent modulus corresponding to the time to failure in the fracture experiment; i.e. the time required to go from the initial loading to the failure point [8]. For the constant cross-head-speed fracture tests conducted here, the times to failure ranged from 20 to a few hundred seconds. In the stress relaxation experiments, the modulus was found to vary by only a few percent over that range. In Fig. 4 for example, the modulus values calculated at the end of the loading ramp (10 s) and just before the unloading ramp (300 s) are shown, and the drop in modulus is less than 2%. Consequently, the remainder of this paper will utilize moduli obtained by averaging the data at the completion of the loading ramp and just before the unloading ramp.
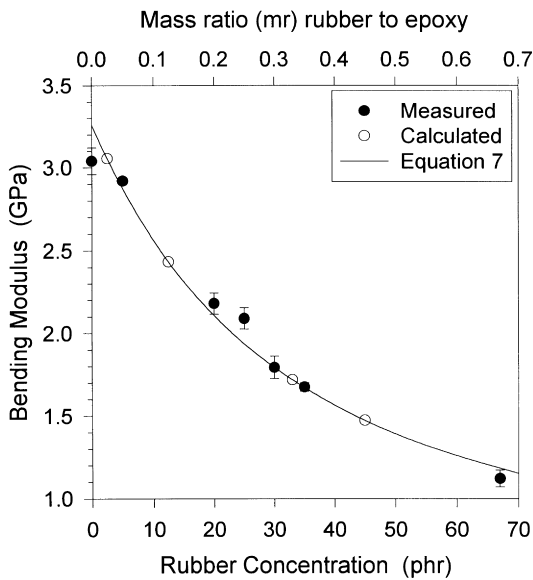
Fig. 5. Bending modulus versus rubber concentration for XU-71790.04L acrylic-modified epoxy dispersions. Error bars represent standard uncertainty in the data.
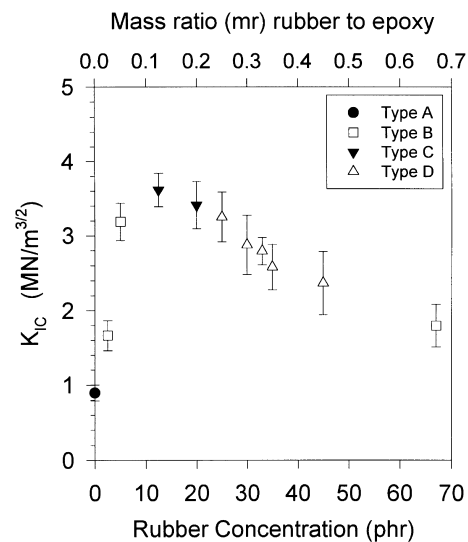

Fig. 6. Critical stress intensity factor versus rubber concentration for XU-71790.04L acrylic-modified epoxy dispersions. Error bars represent standard uncertainty in the data.

Fig. 4 also shows the values of the moduli obtained by ramping to different initial loads prior to the hold. For these data, the maximum strain, ε_m, varies from 0.6 to 2.2%, and the response is linear over this range. The remainder of the bending experiments were conducted at intermediate strains ($\varepsilon_m \sim 1\%$) so the behavior should be linear. Fig. 4 also indicates the uncertainty in the modulus measurements for a single sample, two standard deviations are less than 5%.

The bending modulus was measured as a function of elastomer concentration, and the results are shown in Fig. 5. Each data point is an average of three samples. As expected, the modulus falls with increased elastomer concentration. The data were found to follow the simple relationship:

$$\log E = (\log E_e)(1 - V_r) + (\log E_r)(V_r) \qquad (7)$$

where E, E_r, E_e are the bending moduli of the rubber modified epoxy, the rubber itself, and the unmodified epoxy, while V_r is the volume fraction of rubber in the modified system. Although V_r is not known, it can be approximated based on the known density of the simple epoxy (1.15 g/cm^3), an estimated density for the rubber (1.0 g/cm^3), the weight fractions of epoxy and rubber, and the assumptions that the volume fractions are additive and the contribution of the curing agent can be ignored. The best fit curve is shown in Fig. 5. Modulus values were obtained at only seven of the 11 concentrations used in the fracture experiments. Eq. (7) was used to calculate estimates for the modulus at the other four concentrations.

4.3. Concentration effect on fracture toughness

Values of K_{IC} and G_{IC} for various acrylic rubber-modified epoxy systems are shown in Figs 6 and 7. The results

presented are averages from measurements on 10 samples. The uncertainties shown in the figure correspond to ± 1 standard deviation. When crack growth was unstable, the values corresponded to the onset of rapid crack growth. For those samples that exhibited stable crack propagation, the load was monitored at a series of crack lengths so toughness could be calculated as a function of crack growth. The focus was on the steady crack growth region and not the details of the initiation process. Consequently, although some resistance curve behavior may have been present, the numbers here correspond to crack propagation. It was found that the growth occurred at an approximately constant value for K_I or G_I. This is illustrated in Fig. 8 which shows a typical result for such a sample.

The critical stress intensity factor is plotted as a function of acrylic rubber concentration in Fig. 6. The unmodified epoxy has a comparatively low value of K_{IC}, a reflection of poor crack growth resistance of the amorphous high cross-linked epoxy system. With the addition of 5 phr (0.05 mr) acrylic rubber, there is a steep increase in K_{IC} for the composite. Increasing the rubber dispersion concentration to 12.5 phr (0.125 mr), results in a composite with a maximum K_{IC}. Any further addition of acrylic rubber up to 25 phr (0.25 mr), does not substantially change the K_{IC} of the composite. Beyond 25 phr (0.25 mr), the K_{IC} is found to steadily decrease with increase in rubber concentration.

Fig. 7 illustrates the dependence of fracture toughness on acrylic rubber concentration in the modified epoxy. The trend is similar to that in Fig. 6 but is slightly modified by the change in modulus (see Eq. (6)). Since the modulus falls off as the concentration is increased, the maximum in Fig. 7 is slightly larger and shifted to a slightly higher concentration while the fall off in toughness at higher concentrations is slightly more gradual than would be the case if the modulus did not change.
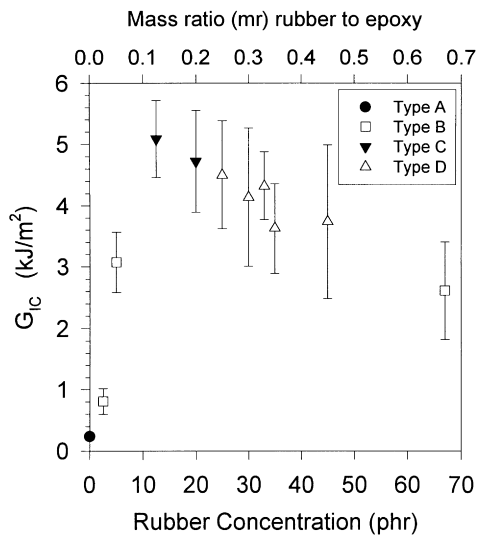
Fig. 7. Fracture energy versus rubber concentration for XU-71790.04L acrylic-modified epoxy dispersions. Error bars represent standard uncertainty in the data.

4.4. Differential scanning calorimetry of modified and unmodified epoxy

The DSC experiments indicated that over the temperature range from −150 to 150°C, two deflections were observed for the unmodified epoxy: a broad low temperature transition at ~ − 60°C and a high temperature transition at 89°C. These correspond to the known positions of the beta relaxation and the glass transition temperature for this epoxy when cured with piperidine for 16 h at 120°C. The rubber modified epoxies gave similar results. A separate deflection for the glass transition of the acrylic elastomer was not observed, but may be hidden by the epoxy's beta relaxation. Fig. 9 illustrates the temperature for the glass transition of the matrix as a function of acrylic-rubber concentration. The
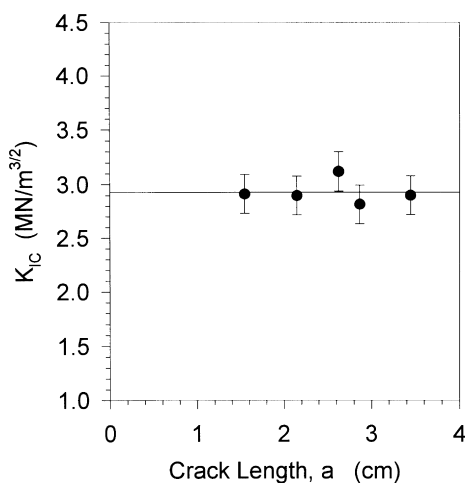

Fig. 8. Critical stress intensity factor as a function of crack length for stable crack growth in a sample with 33 phr (0.33 mr) rubber. Error bars represent standard uncertainty in the data.
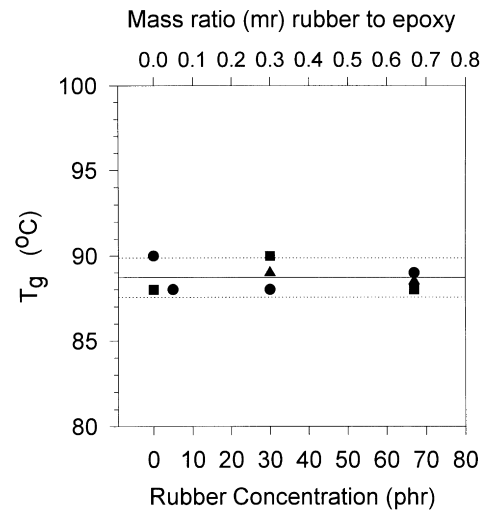

Fig. 9. Glass transition temperature as a function of rubber concentration for acrylic-modified epoxy dispersions. Error bars represent standard uncertainty in the data.

results are plotted for second scans. The data show that the glass transition temperature remains relatively unchanged over the whole range of rubber concentrations. Assuming that the cure process was uniform and similar for all samples, this suggests that the phase separation was very good and did not change as the rubber concentration was increased. Typically, fabrication of toughened materials, like CTBN–epoxy, involve phase separation of the rubber during cure. Inevitably the phase separation is not perfect and some rubber remains in the epoxy matrix and lowers the glass transition temperature. The degree to which this happens can depend on many factors including the cure cycle and the concentration of rubber. In a number of cases, the glass transition temperature falls as the rubber concentration is increased. Consequently, the results in Fig. 9 are very encouraging since they are consistent with the idea that the morphology of the system remains constant and only the density of particles changes as the rubber concentration is increased.

4.5. Microstructural studies

Another way to examine the microstructure is microscopy. Fig. 10 shows micrographs for 5 phr (0.05 mr), 20 phr (0.2 mr), 25 phr (0.25 mr), and 67 phr (0.67 mr) rubber-modified epoxies of specimens obtained by microtoming and staining. The pictures clearly show the two-phase morphology of a composite and indicate that no phase inversion has occurred: i.e. the rubber is always the particle phase while the matrix is the epoxy. There is a good dispersion of particles at all concentrations. Without more analysis, it is impossible to quantify the morphology (particle size and size distribution), but the photographs are consistent with particles in the range from 0.1 to 1.0 μm with an average size of 0.5 μm. More importantly, any large change in morphology with increasing
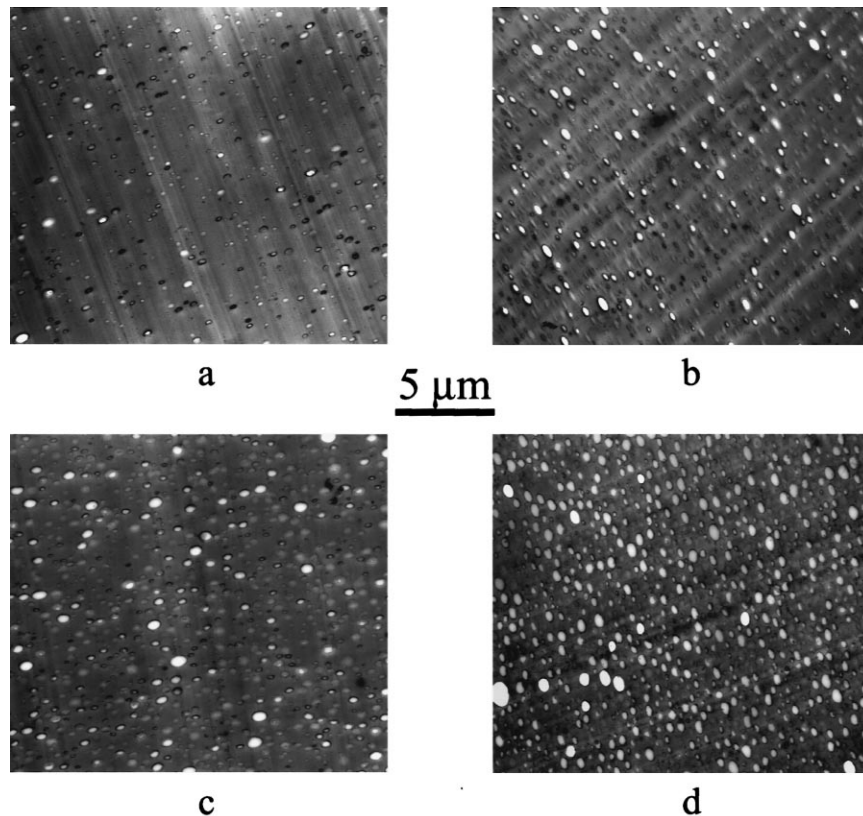
Fig. 10. Micrographs of stained sections for samples with (a) 5 phr (0.05 mr), (b) 20 phr (0.2 mr), (c) 25 phr (0.25 mr), and (d) 67 phr (0.67 mr) rubber.

concentration could be seen in these photographs, and clearly it isn't. Thus all of the evidence supports the idea of a constant particle size and size distribution for all samples.

Fig. 11 shows micrographs of fracture surfaces for samples with 0 phr (0 mr), 5 phr (0.05 mr), 30 phr (0.3 mr), and 67 phr (0.67 mr) rubber. The micrographs are in the region where the initiation of crack growth occurred. As is common in such systems, this region of the fracture surface in the rubber-modified material shows a large number of holes where the rubber particles have cavitated [8]. In some of the holes the rubber particles can be seen suggesting failure at the matrix–particle interface. The pictures also show a clear trend in the appearance of the fracture surfaces. The unmodified epoxy (Fig. 11a) exhibits only minor yielding and plastic deformation as expected for a relatively brittle system. In contrast, the initiation region on the fracture surface for the 5 phr (0.05 mr) material (Fig. 11b) shows significant deformation although it isn't totally pervasive. Similarly, in the 30 phr (0.3 mr) system (Fig. 11c), the entire initiation region displayed large deformations, and there is evidence of yielding on multiple levels. The 67 phr (0.67 mr) sample (Fid. 11d) gave a distinctly different surface. The deformation was wide spread but less severe than that in the 30 phr (0.3 mr) sample. Although the density of particles in the fracture surface was much higher, the fraction that had cavitated to produce holes was much smaller than it was in the 30 phr (0.3 mr)

sample. These observations are consistent with the fracture toughness data for these materials.

4.6. Implications for mechanisms

As mentioned previously, one of the interesting questions in toughened systems is why the fracture energy goes down at higher concentrations. The data here clearly show that loss of morphology is not the answer. The concentration dependence is similar to that observed for other systems, like the CTBN–epoxy materials, even though the acrylic toughened epoxy is able to maintain its morphology over the entire concentration range. The most commonly accepted mechanism for toughening in such materials indicates that the second phase particles act to initiate and assist yielding and plastic flow in the matrix material [21–24]. The argument has been that if you increase the number of particles, more yielding is initiated over a larger area so the toughness goes up. If one extends this argument to it's limits, however, eventually a point must be reached where there simply isn't enough matrix left to have a big effect. When viewed in this way, one would expect that the toughness must go through a maximum as the concentration is increased. Consequently, the results here are perfectly consistent with the current ideas about the mechanism of toughening. Moreover, the data provide a challenging test of any mechanism that proposes a quantitative explanation for toughening.
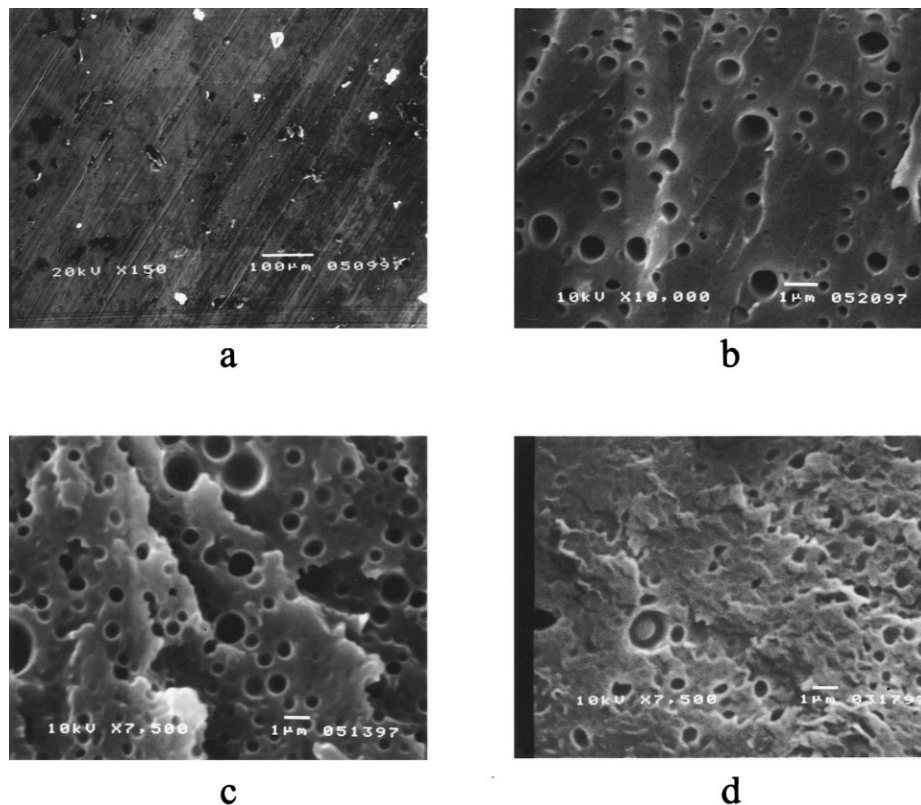
Fig. 11. Scanning electron micrographs of the initiation regions on fracture surfaces of failed specimens with (a) 0 phr (0 mr), (b) 5 phr (0.05 mr), (c) 30 phr (0.3 mr), and (d) 67 phr (0.67 mr) rubber.

5. Conclusions

The following conclusions can be drawn from the current work:

1. The toughness of the epoxy is dramatically improved by the addition of a small amount of acrylic rubber in the form of micrometer size particles. The fracture energy reaches a maximum and remains relatively constant between 12.5 phr (0.125 mr) and 25 phr (0.25 mr) of the rubber. At higher rubber concentrations, the toughness drops gradually but continuously. The fracture behavior changes from unstable to stable as the concentration of rubber is increased, but at the higher concentration of rubber, the crack growth becomes unstable again.
2. The glass transition temperature of the matrix phase remains unchanged over the entire concentration range studied: 0 phr (0 mr) to 67 phr (0.67 mr) rubber. This suggests that the phase separation is very good as might be expected for a system made from preformed rubber particles.
3. Microscopy studies show that the toughened system has two phases with particles that are well dispersed in the epoxy matrix. Although only measured qualitatively, no obvious change in rubber morphology (particle size and size distribution) was seen over the entire range of concentrations studied. The fracture surface in the area of crack growth initiation shows deformation and plastic flow. The magnitude and extent of the deformation correlate with fracture toughness in that both exhibit a maximum in the range of 12.5 phr (0.125 mr) to 25 phr (0.25 mr) rubber.
4. This general trend in fracture behavior as a function of concentration is similar to that seen with other toughened materials like the CTBN–epoxy system. Contrary to previous speculation, however, this trend cannot be attributed to major changes in morphology since that remains relatively constant here.

References

[1] Bolger JC. In: Patrick RL, editor. Treatise on adhesion and adhesives, Vol. 2. New York: Marcell Dekker, 1973:1.

[2] Sultan JN, Laible RC, McGarry FJ. J Appl Polym Sci 1971;;6:127.

[3] Sultan JN, McGarry FJ. Polym Eng Sci 1973;13:29.

[4] Bascom WD, Timmons CO, Jones RL, Peyser PJ. J Appl Polym Sci 1975;19:2545.

[5] Riew CK, Gillham CK. Rubber-modified thermoset resins, Advances in Chemistry Series No 208. Washington, DC: American Chemical Society, 1984.

[6] Riew CK. Rubber-toughened plastics, Advances in Chemistry Series No 222. Washington, DC: American Chemical Society, 1989.

[7] Riew CK, Kinloch AJ. Toughened plastics I, science and engineering, Advances in Chemistry Series No 233. Washington, DC: American Chemical Society, 1993; and Toughened plastics II, novel approaches in science and engineering, Advances in Chemistry Series No 252. Washington, DC: American Chemical Society, 1996.

[8] Bascom WD, Hunston DL. Fractures of elastomer-modified epoxy polymers: a review, Advances in Chemistry Series No 222. Washington, DC: American Chemical Society, 1989.

[9] Kwon O, Ward TC, Morphology development of rubber-modified epoxy thermosets. In: Proc. 19th Annual Meeting of the Adhesion Society, South Carolina, 1996:161.

[10] Kinloch AJ. Relationship between the microstructure and fracture behavior of rubber-toughened thermosetting polymers, Advances in Chemistry Series No 222. Washington, DC: American Chemical Society, 1989.

[11] Hoffman DK, Kolb GC, Arends CB, Stevens MG. Polym Prep Am Chem Society Div of Polym Chem 1985;26 (1):232.

[12] Hoffman DK, Arends CB. Stable dispersion of polymers in polyepoxides. US Patent 4,708,996 (Nov. 24, 1987) (Dow Chemical Company).

[13] Hoffman DK, Oritz C, Hunston DL, McDonough WG. Polym Mater Sci Eng 1994;70:7.

[14] Ortiz C, Hunston DL, McDonough WG, Hoffman DK. Polym Mater Sci Eng 1994;70:9.

[15] Hoffman DK, Kolb GC. Polym Mater Sci Eng 1990;63:593.

[16] Meeks AC. Polymer 1974;15:675.

[17] Kelly FN, Ptak K. Personal communication, 1983.

[18] Pocius AV, Schultz WJ, Adam RE. Proc. Adhesion Society, 1986, p. 4.

[19] Pocius AV. Third generation two-party epoxy adhesives. Proc Int SAMPE Tech Conf 1987;19:312.

[20] Whitney JM, Daniel IM, Pipes RB. Experimental mechanics of fiber reinforced composite materials. Borrkfield Center, CT: Society for Experimental Stress Analysis, 1982:168.

[21] Kinloch AJ, Shaw SJ, Tod DA, Hunston DL. Polymer 1983;24:1341.

[22] Kinloch AJ, Shaw SJ, Tod DA, Hunston DL. Polymer 1983;24:1355.

[23] Yee AF, Pearson RA. J Mater Sci 1986;21 (7):2462.

[24] Pearson RA, Yee AF. J Mater Sci 1986;21 (7):2475.